Monte Carlo Simulations of the Liquid−Vapor Interface of Lennard−Jones Diatomics for the Direct Determination of the Interfacial Tension Using the Test-Area Method†

José G. Sampayo,‡ Felipe J. Blas,§ Enrique de Miguel,§ Erich A. Müller,‡ and George Jackson*,‡

Department of Chemical Engineering, Imperial College London, South Kensington Campus, London SW7 2AZ, U.K., and Departmento de Física Aplicada, Facultad de Ciencias Experimentales, Universidad de Huelva, 21071 Huelva, Spain

We have performed Monte Carlo simulations to examine the vapor−liquid interface of systems of homonuclear diatomic Lennard−Jones (LJ) molecules. The test-area (TA) method developed by Gloor et al. (*J. Chem. Phys.*, **2005**, *123*, 134703) is used to determine the vapor−liquid interfacial tension; the coexistence properties, such as densities and vapor pressures, are also reported. The TA method involves a thermodynamic (free energy perturbation) route to the tension which from a computational point of view offers some advantages over the more common mechanical (virial) route of Kirkwood and Buff (*J. Chem. Phys.* **1949**, *17*, 338). Simulation data are reported for LJ diatomics with different bond lengths $L^* = L/\sigma = 0.3292$, 0.505, 0.6, 0.63, 0.67, 0.793, and 1.0 (with σ representing the diameter of a LJ segment) over the whole range of liquid−vapor coexistence temperatures. The simulated vapor−liquid interfacial tensions for systems with values of the parameters chosen to represent real fluids (e.g., nitrogen, fluorine, chloride, and ethane) are in very good agreement with the experimental data.

1. Introduction

The evaluation of interfacial properties is key in many industrial processes and biological phenomena. From a more fundamental point of view, the understanding of interfacial behavior between a liquid and a vapor phase is of central importance in the description of physical phenomena, for example, capillarity, surfactant behavior, and adhesion between surfaces and liquid droplets. The interfacial tension between a liquid and a vapor can be measured experimentally in a straightforward manner, although certain limitations are encountered, particularly for low values of the tension. A detailed discussion of the various theoretical and computational approaches has been presented by Rowlinson and Widom[1] in their excellent monograph. The most successful theories include the square gradient theory (SGT), originating from the early work of van der Waals[2] and Rayleigh[3] as rediscovered by Cahn and Hilliard,[4] and the more recent approaches based on density functional theory (DFT), as popularized for fluid systems by Evans[5] and others. Fluid interfaces have been simulated at the microscopic level since the early days of the development of the Monte Carlo (MC) and molecular dynamics (MD) techniques which followed the introduction of electronic computers. A number of the key contributions in the area can be attributed to Rowlinson and co-workers including seminal studies of vapor−liquid interfaces for both planar surfaces[6,7] and drops.[8] It is thus a particularly honor for us to present our work in a Special Issue of the *Journal of Chemical and Engineering Data* dedicated to Sir John, who has made such important fundamental advances in broad areas of experimental, theoretical, and simulation research of fluids and fluid mixtures.

There are various options for the determination of the surface tension of fluid interfaces by molecular simulation; the reader is directed to ref 9 for a recent review of the common techniques. We only provide a brief discussion here, highlighting some of the important issues. The most widely employed method to calculate the surface tension is based on a mechanical route, which was first introduced by Kirkwood and Buff.[10] According to the mechanical approach, the surface tension, γ, can be obtained from the appropriate tensorial components of the pressure as

$$\gamma = \int_{-\infty}^{\infty} [P_N - P_T(z)]\, dz \quad (1)$$

where P_N is the component of the pressure tensor normal to the surface, while P_T is the tangential component. Here, the z direction is taken to be orthogonal to the plane of the interface. An alternative methodology for the calculation of surface tension is the finite size scaling approach introduced by Binder,[11] usually implemented in the grand canonical ensemble; the advantage of this approach is that one can estimate values of the interfacial tension close to the critical point. The other class of technique is based on a thermodynamic route where the surface contribution to the free energy is evaluated directly from a perturbative scheme. The test-area (TA) method,[9] which has gained popularity in recent years, belongs to this class of thermodynamic approaches.

At first sight the TA method for the direct determination of interfacial tension bears much resemblance to the approach of Bennett[12] for the calculation of the difference in free energy from the simultaneous simulation of two (or more) distinct systems; if the systems have different interfacial areas, one can estimate the corresponding surface tension (and surface free energy).[13,14] In the case of the TA approach, however, the

† Part of the "Sir John S. Rowlinson Festschrift".

* Corresponding author. E-mail: g.jackson@imperial.ac.uk.
‡ Imperial College London.
§ Universidad de Huelva.

10.1021/je100450s
Published on Web 07/19/2010

derivative of the free energy with respect to the interfacial area is estimated directly (using a finite difference method) from the simulation of a single (inhomogeneous) system by computing the change in free energy due to small test (ghost) perturbations in the area; the change in free energy is determined from the general perturbation expressions developed by Zwanzig.[15] One should note that there is a close similarity between the TA formalism and related approaches employing the so-called expanded ensemble[16,17] and wandering interface[18] methods. Detailed comparisons of the various methods were made by Errington and Kofke.[16]

The change in the Helmholtz free energy F of a system in the canonical ensemble (where the number of particles N, volume V, and temperature T are held constant) due to a perturbation from a state 0 to a state 1 can be defined in terms of the corresponding partition functions Q_0 and Q_1 as

$$\Delta F_{0\rightarrow 1} = F_1 - F_0 = -k_B T \ln\left(\frac{Q_1}{Q_0}\right) = -k_B T \ln\left(\frac{Z_1}{Z_0}\right) \tag{2}$$

where k_B is the Boltzmann constant, and the partition function is

$$Q = \frac{1}{N!\Lambda^{3N}} \int \exp\left(-\frac{U}{k_B T}\right) \mathrm{d}\mathbf{r}^N = \frac{Z}{N!\Lambda^{3N}} \tag{3}$$

Here, $Z = \int \exp(-U/k_B T)\, \mathrm{d}\mathbf{r}^N$ is the configurational integral, $U(\mathbf{r}^N)$ is the configurational energy which is a function of the configurational space $\mathbf{r}^N$ (and corresponds to the total potential energy resulting from the interactions between all of the particles in the system in the absence of external fields), and Λ is the de Broglie wavelength which incorporates all of the kinetic contributions. If the configurational energy U_1 of state 1 is treated as a perturbation to the initial configurational energy U_0 ($U_1 = U_0 + \Delta U$, where ΔU is the change in the potential energy due to the perturbation), then the ratio of configurational integrals in eq 2 can be expressed as

$$\frac{Z_1}{Z_0} = \frac{\int \exp\left(-\frac{U_1}{k_B T}\right) \mathrm{d}\mathbf{r}^N}{\int \exp\left(-\frac{U_0}{k_B T}\right) \mathrm{d}\mathbf{r}^N} = \frac{\int \exp\left(-\frac{U_0}{k_B T}\right) \exp\left(-\frac{\Delta U}{k_B T}\right) \mathrm{d}\mathbf{r}^N}{\int \exp\left(-\frac{U_0}{k_B T}\right) \mathrm{d}\mathbf{r}^N} \tag{4}$$

The probability of a particular configuration of N particles being in a state $\mathbf{r}^N$ is proportional to

$$P(\mathbf{r}^N) = \frac{1}{N!\Lambda^{3N} Q} \exp\left(-\frac{U}{k_B T}\right) = \frac{1}{Z} \exp\left(-\frac{U}{k_B T}\right) \tag{5}$$

and the corresponding ensemble average of any property M is thus given by

$$\langle M \rangle = \int M\, P(\mathbf{r}^N)\, \mathrm{d}\mathbf{r}^N = \frac{1}{Z} \int M \exp\left(-\frac{U}{k_B T}\right) \mathrm{d}\mathbf{r}^N \tag{6}$$

so that eq 4 can be expressed as the Boltzmann factor of the change ΔU in configurational energy averaged over the unperturbed system 0:

$$\frac{Z_1}{Z_0} = \left\langle \exp\left(-\frac{\Delta U}{k_B T}\right) \right\rangle_0 \tag{7}$$

Inserting the result of eq 7 in eq 2 for the perturbation in the Helmholtz free energy ΔF we obtain the following simple relation:

$$\Delta F_{0\rightarrow 1} = -k_B T \ln\left\langle \exp\left(-\frac{\Delta U}{k_B T}\right) \right\rangle_0 \tag{8}$$

The equation is the general result of Zwanzig[15] that forms the basis of high-temperature perturbation theories; it is important to emphasize at this point that eq 8 is exact in the limit of infinitesimal perturbations.

We now turn to the thermodynamic definition of surface tension which in the case of a planar interface in the canonical ensemble can be expressed as[1]

$$\gamma = \left(\frac{\partial F}{\partial A}\right)_{N,V,T} = \lim_{\Delta A \rightarrow 0} \left(\frac{\Delta F}{\Delta A}\right)_{N,V,T} \tag{9}$$

The TA method consists in performing very small test changes (perturbations) in the interfacial area of the system (by increasing/decreasing the box dimensions in the plane of the interface with a corresponding decrease/increase in the box length normal to the interface) keeping the number of particles N, volume V, and temperature T constant. The change in Helmholtz free energy due to the test perturbation in the area is obtained from eq 8 as the Boltzmann factor of the test change in the configurational energy averaged over the configurations of the unperturbed reference system. The surface tension can then simply be estimated from eq 9 from an extrapolation to infinitesimal area perturbations:

$$\gamma = \lim_{\Delta A \rightarrow 0} \left(\frac{\Delta F_{0\rightarrow 1}}{\Delta A}\right)_{N,V,T} = \lim_{\Delta A \rightarrow 0} \frac{-k_B T \ln\left\langle \exp\left(-\frac{\Delta U}{k_B T}\right) \right\rangle_0}{\Delta A} \tag{10}$$

A similar form of the Zwanzig relation is commonly used to estimate the chemical potential with test perturbations in the number of particles (c.f., the test-particle method of Widom[19]) or to determine the pressure[20−22] and pressure tensor[23,24] with test-volume perturbations.

Originally, the TA approach was implemented in combination with Metropolis MC simulations to determine the surface tension for the vapor−liquid interface of Lennard−Jones (LJ) and square-well systems.[9] The estimates obtained with the TA method were found to be in good agreement with those obtained from a mechanical route and MD simulation. The TA method and its variants have been used extensively to determine the interfacial tensions of systems with realistic potentials, for example, *n*-alkanes,[25] water,[26] binary mixtures of *n*-alkanes,[27]

high-pressure aqueous solutions of methane[28] and acid gases,[29,30] ionic liquids,[31] and model fluids including chains of LJ segments,[17,32,33] the Widom−Rowlinson mixture,[34] Mie $n-6$ particles,[35] and drops of LJ fluids.[36] The method is now also being extended to treat the fluid−fluid and fluid−solid interfaces exhibited by systems with hard-core interactions such as hard-sphere chains,[37,38] primitive models of liquid crystals,[39−42] model colloid−polymer mixtures,[43,44] and mixtures of prolate and oblate particles.[45,46]

In the original work with the TA approach,[9] the central difference (CD) approximation was taken from two simultaneous test perturbations from the reference state to provide more accurate values for the surface tension; the first deformation involved an increase in the surface area $A_1 = A_0 + \Delta A$ corresponding to a free-energy change of $\Delta F_{0\rightarrow 1} = F_1(A_1) - F_0(A_0)$, and the second a decrease in the surface area $A_{-1} = A_0 - \Delta A$ corresponding to a free-energy change of $\Delta F_{0\rightarrow -1} = F_{-1}(A_{-1}) - F_0(A_0)$.

In the current work we study the vapor−liquid interfacial tension obtained with the TA method from MC simulations of the vapor−liquid equilibria (VLE) of two center homonuclear LJ molecules (2CLJ) for a range of bond lengths. Accurate estimates for the surface tension are obtained from an extrapolation to infinitesimal area changes $\Delta A = 0$ from a linear fit of the average of the results obtained from a series of positive and negative perturbations in the surface area. Our results are compared with those obtained by other techniques where possible. A comparison with experimental results of real diatomic fluids is also made using values of intersegment parameters from the literature.

2. Simulation of the Interfacial Tension

The 2CLJ diatomics studied here comprise two spherically truncated sites characterized by a 12−6 LJ site−site potential with a cutoff radius of 6σ:

$$u_{\mathrm{ST}}(r) = \begin{cases} 4\varepsilon\left[\left(\frac{\sigma}{r_{ij}}\right)^{12} - \left(\frac{\sigma}{r_{ij}}\right)^{6}\right] & r_{ij} \le 6\sigma \\ 0 & r_{ij} > 6\sigma \end{cases} \qquad (11)$$

where σ is the diameter of each site, ε is the well-depth energy parameter, and r_{ij} is the distance between site i of one molecule and site j on another. No long-range corrections are considered as these are negligible for this range of interaction.[9,47,48] The variables are described in reduced units for convenience, being defined in terms of the LJ size and energy parameters: the bond length $L^* = L/\sigma$, the temperature $T^* = k_B T/\varepsilon$, the density $\rho^* = \rho\sigma^3$, the pressure $P^* = P\sigma^3/\varepsilon$, the energy $E^* = E/\varepsilon$, the surface tension $\gamma^* = \gamma\sigma^2/\varepsilon$, the box dimensions $l^* = l/\sigma$, the interface area $A^* = A/\sigma^2$, the distance from the interface $z^* = z/\sigma$, and the interface width $D^* = D/\sigma$.

The vapor−liquid coexistence of systems of 2CLJ with bond lengths L^* of 0.3292, 0.505, 0.60, 0.63, 0.67, 0.793, and 1.0 is considered. Metropolis Monte Carlo simulations (MC-*NVT*)[49] are carried out in elongated boxes of dimensions $V = l_x \times l_y \times l_z = 17.5\sigma \times 17.5\sigma \times 52.5\sigma$. Periodic boundary conditions are used in each direction. The number of particles N is chosen so that ρ is close to the critical density in each system. We perform the MC analogue of a temperature quench spinodal separation,[50] and the system is equilibrated for at least $5\cdot 10^5$ cycles until the liquid and vapor phases are separated by two interfaces. A cycle consists in N trial particle moves, where a move can be either translational or orientational with the same probability. The magnitude of the particle moves is adjusted to give a ~30 % to 35 % acceptance rate. Runs are performed for each system at temperatures ranging from $T_r = T/T_c = 0.5$ to 0.95 (where T_c is the critical temperature), with increments of $\Delta T^* = 0.1$. For each new temperature, $2.5\cdot 10^5$ equilibration cycles are performed followed by $5\cdot 10^5$ production cycles.

A density profile along the long axis of the simulation box is obtained for each temperature. For this purpose, the simulation cell is divided into a histogram over 1050 slabs along the z direction. The vapor and liquid coexistence densities, ρ_v^* and ρ_l^*, are determined directly from the density profiles, taking averages in regions sufficiently removed from the interface. Estimates of the errors of the coexistence densities are computed as the standard deviations from the mean densities. The reduced interfacial thickness D^* and the position of the Gibbs dividing surface z_0 are obtained from a fit of the density profiles to the following algebraic expression:

$$\rho^*(z^*) = \frac{1}{2}(\rho_l^* + \rho_v^*) - \frac{1}{2}(\rho_l^* - \rho_v^*)\tanh\left(\frac{z^* - z_0^*}{D^*}\right) \qquad (12)$$

In Table 1 we compile the VLE data obtained for each system after equilibration, including the saturation temperature T^*, vapor pressure P_v^*, coexistence densities for the liquid and the vapor phases, ρ_l^* and ρ_l^*, and interfacial thickness D^*. The coexistence envelopes for the various systems are depicted in Figure 1 and compared with the data reported by Dubey et al.[51] and Kriebel et al.[52] obtained from MD simulations, showing good agreement. The MD data of Kriebel et al. extend to higher temperatures (possibly due to system size effects and the expected overestimate of the critical point) and are confined to a narrower range of temperatures. The density-profile data from our MC simulations for the 2CLJ system with a bond length of $L^* = 0.6$ for temperatures ranging from $T^* = 1.4$ to 2.2 are compared with the hyperbolic tangent description of eq 12 in Figure 2; a small degree of structure is seen in the dense phase close to the interface for the lowest temperature examined. The temperature dependence of the interfacial width D^* is shown in Figure 3 for different values of L^*; the maximum interfacial width exhibits an inverse correlation with the bond length. At low temperatures, the same sharp interface, with $D^* \approx 0.5$, is observed for the systems with the various bond lengths. The vapor pressure is calculated using the virial route[49] by undertaking separate MC-*NVT* simulations of homogeneous systems at the corresponding vapor densities. To correlate the coexistence densities, the phase equilibrium data are fitted to the following expression as in ref 53:

$$\rho_{\pm} = \rho_c + C_2\left|1 - \frac{T^*}{T_c^*}\right| \pm \frac{1}{2}B_0\left|1 - \frac{T^*}{T_c^*}\right|^{\beta} \qquad (13)$$

Here, β is set to its universal value ($\beta = 0.325$, as determined from renormalization group theory), ρ_+ and ρ_- represent the vapor and liquid phase densities, respectively, and C_2 and B_0 are adjustable parameters, the optimal values of which are reported in Table 2 together with the corresponding values of the critical temperature and density. The critical pressure P_c is calculated from eq 14 with the corresponding value of the critical temperature:

$$\ln P_v^* = a + b/(T^* + c) \qquad (14)$$

Table 1. Reduced Temperature (T^*), Vapor Pressure (P_v^*), Vapor and Liquid Coexistence Densities (ρ_l^* and ρ_v^*), Interfacial Width (D^*), and the Surface Tension (γ^*) for the VLE of 2CLJ Fluids for Various Bond Lengths L^* Obtained from MC-*NVT* Simulations and the TA Method[a]

T^*	P_v^*	ρ_l^*	ρ_v^*	D^*	γ^*
		$L^* = 0.3292$			
		$N = 3790$			
1.8	0.0012561(1)	0.659(2)	0.0007(1)	0.658	2.651(38)
1.9	0.0026009(4)	0.648(3)	0.0014(1)	0.706	2.478(63)
2.0	0.0049666(7)	0.634(2)	0.0026(2)	0.775	2.282(54)
2.1	0.007478(1)	0.622(2)	0.0037(1)	0.865	2.099(51)
2.2	0.010464(2)	0.609(2)	0.0050(1)	0.944	1.896(27)
2.3	0.016291(5)	0.596(2)	0.0076(2)	1.017	1.724(38)
2.4	0.021535(8)	0.583(2)	0.0098(2)	1.156	1.538(42)
2.5	0.03124(1)	0.567(2)	0.0141(6)	1.317	1.365(37)
2.6	0.03931(2)	0.552(2)	0.0174(4)	1.444	1.195(29)
2.7	0.05125(2)	0.534(1)	0.0225(6)	1.568	1.029(44)
2.8	0.06515(3)	0.515(1)	0.0285(3)	1.731	0.857(44)
2.9	0.08542(4)	0.502(1)	0.0381(3)	1.931	0.708(29)
3.0	0.10366(4)	0.481(1)	0.0466(3)	2.292	0.559(26)
3.1	0.12915(9)	0.463(1)	0.0602(9)	2.486	0.452(54)
		$L^* = 0.505$			
		$N = 3312$			
1.4	0.00084792(6)	0.560(2)	0.0006(1)	0.629	1.890(47)
1.5	0.0017036(3)	0.547(3)	0.0012(1)	0.714	1.726(58)
1.6	0.0036549(6)	0.533(2)	0.0024(2)	0.804	1.553(51)
1.7	0.006058(1)	0.520(2)	0.0037(2)	0.920	1.368(42)
1.8	0.009475(3)	0.504(1)	0.0056(3)	1.048	1.217(32)
1.9	0.013767(4)	0.489(1)	0.0079(5)	1.243	1.032(45)
2.0	0.021744(7)	0.475(2)	0.0123(3)	1.386	0.886(41)
2.1	0.03178(1)	0.456(1)	0.0179(5)	1.536	0.726(39)
2.2	0.04413(2)	0.439(1)	0.0249(5)	1.824	0.587(24)
2.3	0.05960(3)	0.417(1)	0.0341(3)	2.131	0.431(36)
2.4	0.07633(7)	0.398(1)	0.0442(3)	2.481	0.321(28)
2.5	1.0017(1)	0.371(1)	0.062(1)	3.089	0.195(27)
		$L^* = 0.60$			
		$N = 3168$			
1.3	0.00101975(7)	0.513(2)	0.0008(2)	0.677	1.524(67)
1.4	0.0016192(2)	0.499(2)	0.0012(1)	0.818	1.381(32)
1.5	0.0035293(6)	0.484(2)	0.0024(2)	0.941	1.199(45)
1.6	0.007080(1)	0.469(2)	0.0047(3)	1.036	1.055(40)
1.7	0.012330(3)	0.453(2)	0.0080(3)	1.183	0.890(35)
1.8	0.018039(5)	0.436(1)	0.0114(3)	1.380	0.722(48)
1.9	0.02824(1)	0.419(1)	0.0178(3)	1.580	0.597(33)
2.0	0.03894(1)	0.399(1)	0.0244(3)	1.853	0.458(28)
2.1	0.05447(6)	0.378(1)	0.0349(8)	2.256	0.316(33)
2.2	0.07190(5)	0.353(1)	0.0474(3)	2.962	0.197(22)
2.25	0.0860(1)	0.340(1)	0.0604(4)	3.313	0.157(31)
		$L^* = 0.63$			
		$N = 2894$			
1.2	0.00047601(6)	0.511(2)	0.00040(7)	0.642	1.559(44)
1.3	0.0015805(3)	0.496(2)	0.0012(1)	0.693	1.417(52)
1.4	0.0026909(7)	0.482(2)	0.0020(2)	0.834	1.269(49)
1.5	0.004396(1)	0.467(2)	0.0031(4)	1.005	1.092(27)
1.6	0.008534(1)	0.452(1)	0.0058(2)	1.124	0.935(32)
1.7	0.014408(6)	0.434(2)	0.0095(2)	1.283	0.795(29)
1.8	0.021896(8)	0.417(1)	0.0142(3)	1.533	0.613(12)
1.9	0.03276(2)	0.399(1)	0.0212(5)	1.800	0.499(29)
2.0	0.04607(2)	0.376(1)	0.0302(8)	2.123	0.359(28)
2.1	0.06352(3)	0.351(1)	0.0433(3)	2.616	0.230(22)
2.2	0.0855(1)	0.318(1)	0.063(1)	3.350	0.126(28)
		$L^* = 0.67$			
		$N = 2846$			
1.2	0.0010741(2)	0.490(3)	0.0009(1)	0.636	1.419(59)
1.3	0.0016953(2)	0.475(2)	0.0013(2)	0.805	1.276(46)
1.4	0.0040594(9)	0.461(2)	0.0030(4)	0.869	1.091(36)
1.5	0.006988(1)	0.446(2)	0.0050(3)	1.041	0.923(30)
1.6	0.009745(2)	0.429(1)	0.0066(3)	1.289	0.803(33)
1.7	0.017947(9)	0.411(1)	0.0121(3)	1.446	0.646(29)
1.8	0.02638(1)	0.391(1)	0.0176(3)	1.744	0.500(40)
1.9	0.03951(2)	0.371(1)	0.0268(7)	2.002	0.362(31)
2.0	0.05433(4)	0.349(1)	0.0377(7)	2.662	0.258(25)
2.05	0.06499(5)	0.332(1)	0.0468(3)	2.859	0.179(34)
2.1	0.07739(9)	0.317(1)	0.0594(9)	3.214	0.142(15)

Table 1. Continued

T^*	P_v^*	ρ_l^*	ρ_v^*	D^*	γ^*
		$L^* = 0.793$			
		$N = 2605$			
1.0	0.00030394(4)	0.467(2)	0.00031(8)	0.545	1.346(25)
1.1	0.00064492(3)	0.451(2)	0.0006(1)	0.716	1.192(24)
1.2	0.0021685(5)	0.436(2)	0.0019(3)	0.789	1.040(23)
1.3	0.0036612(7)	0.420(2)	0.0030(2)	0.919	0.886(25)
1.4	0.007089(2)	0.403(1)	0.0055(3)	1.163	0.732(22)
1.5	0.012964(6)	0.385(1)	0.0098(3)	1.353	0.589(16)
1.6	0.020367(7)	0.366(1)	0.0152(8)	1.686	0.452(26)
1.7	0.03013(2)	0.345(1)	0.0224(4)	2.058	0.325(21)
1.8	0.04582(4)	0.318(1)	0.0358(4)	2.631	0.199(19)
		$L^* = 1.0$			
		$N = 2000$			
0.9	0.00016502(1)	0.421(3)	0.00018(5)	0.605	1.144(41)
1.0	0.0007482(1)	0.405(3)	0.0008(1)	0.737	0.960(24)
1.1	0.0021139(4)	0.389(2)	0.0020(3)	0.880	0.803(32)
1.2	0.004138(1)	0.371(2)	0.0037(3)	1.111	0.661(26)
1.3	0.007953(3)	0.352(1)	0.0068(3)	1.373	0.519(27)
1.4	0.01627(1)	0.331(1)	0.0140(5)	1.623	0.378(21)
1.5	0.02423(1)	0.308(1)	0.0205(8)	2.269	0.256(19)
1.6	0.04129(4)	0.277(1)	0.0389(8)	2.811	0.141(16)

[a] The total number of particles in the parallelepiped cell is N. The errors are estimated from the standard deviation of the mean determined from 10 subaverages of $5 \cdot 10^3$ cycles each. For example, 1.23(4) represents 1.23 ± 0.04.

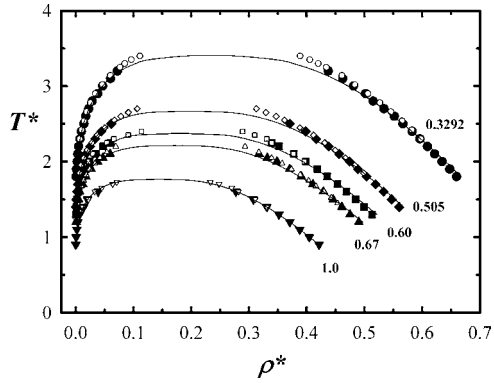

Figure 1. Temperature−density representation of the VLE obtained from MC-*NVT* simulations of 2CLJ fluids for different bond lengths. $L^* = 0.3292$: ●, this work, ○, ref 52; $L^* = 0.505$: ◆, this work, ◇, ref 52; $L^* = 0.60$: ■, this work, □, ref 51; $L^* = 0.67$: ▲, this work, △, ref 52; $L^* = 1.0$: ▼, this work, ▽, 51. The continuous curves correspond to the correlation of eq 13 to our simulation data.

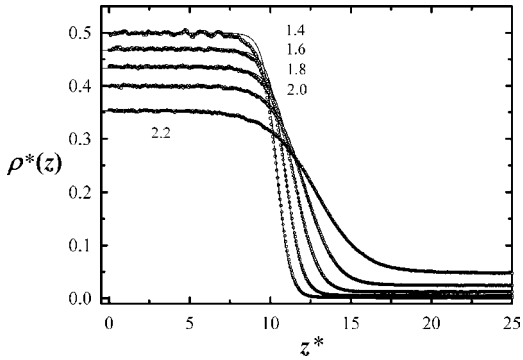

Figure 2. Density profiles of the VLE obtained from MC-*NVT* simulations of 2CLJ fluids for systems with a bond length of $L^* = 0.60$ for five different temperatures (the reduced values of which are labeled on the figure): ○, simulation results; —, eq 12.

Here a, b, and c are obtained by fitting this expression to the vapor pressure data; the optimal values for these parameters are also given in Table 2.

Once equilibrated, the inhomogeneous systems consist of phase-separated vapor and liquid regions in direct contact,

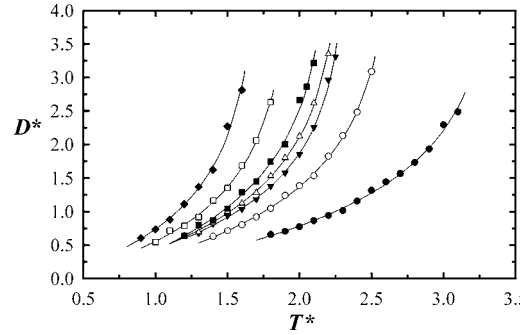

Figure 3. Dependence of the reduced interface width (D^*) on the reduced temperature (T^*) for the VLE obtained from MC-*NVT* simulations of 2CLJ fluids for different bond lengths: ◆, $L^* = 1.0$; □, $L^* = 0.793$; ■, $L^* = 0.67$; △, $L^* = 0.63$; ▼, $L^* = 0.60$; ○, $L^* = 0.505$; ●, $L^* = 0.3292$; —, a temperature dependent correlation.

contained within a parallelepiped simulation box of dimensions $V = l_x l_y l_z$. The elongation of the rectangular box in the z direction, where $3l_x = 3l_y = l_z$, ensures that two vapor−liquid interfaces develop parallel to the $x-y$ plane. The initial equilibrated reference state (0) corresponds to an average interfacial area of $A_0 = 2l_{x,0}l_{y,0}$. The dimensionless perturbation parameter ξ is set at the start of the simulation, and the corresponding small fractional change in the dimensionless area is obtained as $\Delta A^* = A_0^* \xi$. The perturbation is performed in such a way that the scaled dimensions along the x and y axes are increased (or decreased) in the same proportion, that is, $l_{x,1}^* = l_{x,0}^*(1 + \xi)^{1/2} = l_{y,1}^* = l_{y,0}^*(1 + \xi)^{1/2}$. To keep the overall volume constant, the dimension in the z direction is decreased (or increased) accordingly to $l_{z,1}^* = l_{z,0}^*(1 + \xi)^{-1}$. Thus the perturbed state corresponds to a new surface area of $A_1^* = A_0^*(1 + \xi)$.

Positive and negative TA perturbations are undertaken simultaneously once every 10 cycles to evaluate the Boltzmann factors of the difference in configurational energy which are required to determine the change in free energy and thus the surface tension. Once independent values of surface tension for the positive and negative change in surface area are obtained from eq 10 for several values of the perturbation parameter, an average value is calculated for each one. The final estimate of

Table 2. Reduced Critical Temperature T_c^*, Pressure P_c^*, and Density ρ_c^* Obtained from MC-*NVT* Simulations of 2CLJ Fluids for Various Bond Lengths L^* Compared with the MD Values Obtained by Dubey et al.[51] and Kriebel et al.[52] [a]

L^*		T_c^*	P_c^*	ρ_c^*	C_2	B_0	a	b	c
0.3292	MC (this work)	3.4028	0.2110	0.2339	0.2122	0.8510	3.2700	−15.2145	−0.2502
	MD[52]	3.5436		0.24524					
0.505	MC (this work)	2.6664	0.1454	0.1965	0.1839	0.7217	3.7714	−15.2591	0.0108
	MD[52]	2.8001		0.20566					
0.60	MC (this work)	2.3739	0.1163	0.1801	0.1793	0.6742	3.4391	−12.8749	−0.0706
	MD[51]	2.27 ± 0.01		0.197 ± 0.01					
0.63	MC (this work)	2.3156	0.1161	0.1768	0.1665	0.6507	3.8175	−14.0955	0.0451
0.67	MC (this work)	2.2121	0.1079	0.1711	0.1702	0.6397	5.6755	−21.5023	0.5089
	MD[52]	2.3355		0.17526					
0.793	MC (this work)	2.0066	0.08838	0.1588	0.1506	0.5857	3.5285	−12.2067	0.0434
1.0	MC (this work)	1.7638	0.07212	0.1438	0.1368	0.5312	2.7684	−8.8874	−0.1173
	MD[51]	1.78 ± 0.01		0.149 ± 0.01					

[a] The fitted parameters B_0 and C_2 (of eq 13) and a, b, and c (of eq 14) are also included.

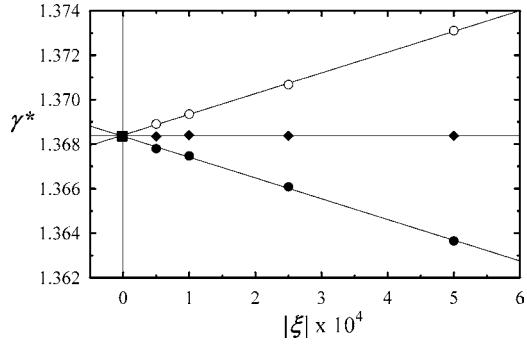

Figure 4. Values of the reduced surface tension of the VLE obtained from MC-*NVT* and the TA approach in simulations of 2CLJ fluids with a bond length of $L^* = 0.505$ at a reduced temperature of $T^* = 1.7$. Data are shown for different values of the perturbation factor: ○, expansive perturbations, $\xi > 0$; ●, compressive perturbations, $\xi < 0$; and ◆, average of the positive and negative perturbations. ■ corresponds to the tension γ^* obtained by extrapolation to infinitesimal perturbations.

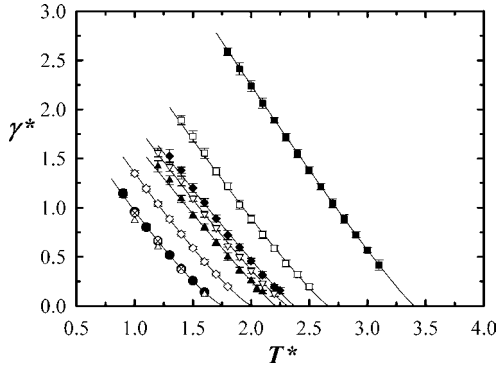

Figure 5. Dependence of the reduced surface tension (γ^*) on the reduced temperature (T^*) for the VLE obtained from MC-*NVT* simulations and the TA method of 2CLJ fluids for different bond lengths: ■, $L^* = 0.3292$; □, $L^* = 0.505$; ◆, $L^* = 0.60$; ▽, $L^* = 0.63$; ▲, $L^* = 0.67$; ◇, $L^* = 0.793$; ●, $L^* = 1.0$ (this work); △, MD;[48] ○, MC expanded ensemble;[17] ×, MC TA;[17] —, correlation of eq 15.

the vapor−liquid interfacial tension is determined from an extrapolation to $\xi \rightarrow 0$ with the linear fit of the averages obtained for the different values of ξ[23] (see Figure 4). The corresponding values of the surface tension are reported in Table 1 and are also depicted in Figure 5 for the 2CLJ systems with the various bond lengths. The errors are obtained by calculating the standard deviation of the mean determined from 10 blocks averages of entire data. The surface tension data obtained from the TA approach are also correlated with the expression of Guggenheim:[54]

$$\gamma^* = \gamma_0(1 - T^*/T_c^*)^{\mu} \qquad (15)$$

Table 3. Parameters Corresponding to the Guggenheim Relation (eq 15) for the Vapor−Liquid Interfacial Tension of 2CLJ Fluids for Various Bond Lengths L^*

L^*	γ_0	μ
0.329	5.946	1.098
0.505	4.310	1.133
0.60	3.508	1.086
0.63	3.538	1.133
0.67	3.176	1.076
0.793	3.110	1.207
1.0	2.755	1.252

Table 4. 2CLJ Bond Length (L^*), Segment Energy (ε), and Size (σ) Parameters for Selected Real Substances

fluid	L^*	ε/k_B (K)	σ (Å)
N_2	0.329	36.67	3.308
F_2	0.505	53.47	2.832
C_2H_6	0.505	112.2	3.64
Cl_2	0.63	178.3	3.332

where γ_0 and μ are seen to provide a good overall description of the tension for these systems; the corresponding values of γ_0 and μ are given in Table 3. One should note that the universal value of $\mu = 1.23$ was not found to provide an adequate representation of the data for the particles with the shorter bond lengths over the entire temperature range. The results corresponding to the tangent LJ diatomic system with $L^* = 1.0$ are compared with existing data,[48,17] and good agreement is apparent.

3. Real Substances

The 2CLJ model has been shown to provide a good representation of the intermolecular potential of small apolar molecules and can be used as a reference for perturbation approaches that incorporate polar[55] or quadrupolar interactions.[56] Here we use the parametrization of the 2CLJ model for real systems and compare the simulation results with the experimental values for the vapor−liquid coexistence densities and surface tension. A number of studies have been carried out to describe the VLE of real substances with 2CLJ systems.[57−64]

We have chosen to examine nitrogen, fluorine, chlorine, and ethane, the site−site LJ parameters for which are given in Table 4, taken from the work of McGuigan et al.[61] and Spyriouni et al.[62] In Figures 6 and 7 we show a comparison of our simulated values for the vapor−liquid coexistence densities and interfacial tension with the corresponding experimental data.[65−67] No attempt has been made to reparameterize the potential parameters or to perform a comparative evaluation of the potential functions. From Figure 6 we can conclude that the potentials used provide a reliable description of VLE densities. From Figure 7 one can also see that there is a good representation of

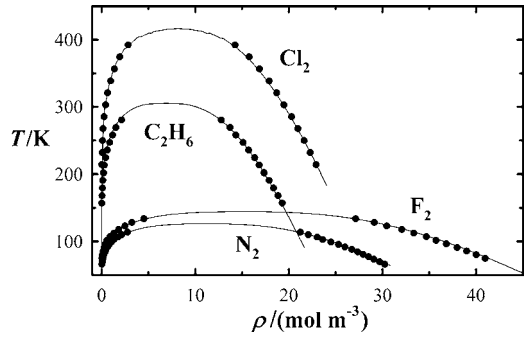

Figure 6. Comparison of the experimental saturated vapor and liquid densities of real fluids with the values obtained from MC-*NVT* simulation of 2CLJ models: ●, model parameters of Table 3; —, correlated experimental data from NIST webbook,[65] and experimental data for Cl_2.[66]

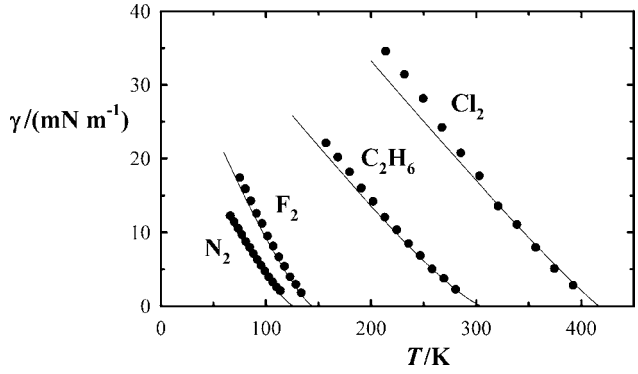

Figure 7. Comparison of the experimental vapor−liquid interfacial tension of real fluids with the values obtained from MC-*NVT* simulation and the TA method of 2CLJ models: ●, model parameters of Table 3; —, correlated experimental data from the NIST webbook[65] for N_2, F_2, and C_2H_6, and Prosim Component Plus[67] for Cl_2.

the vapor−liquid interfacial tension, with a slightly poorer description for chlorine (though in this case we should note that the comparison is with estimated values rather than with actual experimental data). Multipolar interactions arising from the uneven charge distributions in the molecules are not explicitly taken into account in these models but rather averaged into the potential parameters. In addition a united atom coarse-grained representation is made in this case. If interfacial tension data were to be used in the parameter estimation, a more robust description of the experimental data could presumably be achieved. Notwithstanding, these results confirm that simple molecular models such as the 2CLJ are appropriate not only for bulk fluid phase equilibria but also for the interfacial properties. Studies of the fluid phase equilibria and interfacial properties of these types of models for mixtures of *n*-alkanes and *n*-perfluoroalkanes including xenon as a component (the latter taking on the role of an ennobled alkane[68−70]) are currently being undertaken.

4. Conclusions

The TA approach is seen to be an efficient and versatile method to determine the surface tension of molecular systems such as the two center LJ fluids. Vapor−liquid coexistence properties and the interfacial tension of systems of 2CLJ particles have been investigated for a range of physically reasonable bond lengths, covering temperatures over the entire fluid region. A comparison of these data with published results confirmed the adequacy of the approach. The TA method has an advantage over the mechanical approach in that it does not rely on the calculation of the components of the pressure tensor through the use of the virial relation. Its application using MC is therefore straightforward, as only configurational energies are required. We have also shown that simple 2CLJ models can provide a good description of vapor−liquid surface tension of real diatomic fluids such as nitrogen, fluorine, chlorine, and ethane, using potential parameters refined to bulk VLE data alone. As well as providing a good analysis of the adequacy of the intermolecular potential model in describing the thermodynamic properties of real fluids, our simulation data for the 2CLJ systems will be useful in assessing the quality of theoretical developments. In future work we plan to extend the DFT free energy functionals[71−75] developed with the statistical associating fluid theory for potentials of variable range (SAFT-VR)[76,77] to molecules formed from LJ segments. The SAFT-VR formalism originally formulated for bulk fluids of molecules formed from square-well segments is generic and can easily be cast to treat the LJ,[78] Yukawa,[79] and Mie[80] forms of the site−site potential. The 2CLJ data reported in the current work will provide an invaluable test bed for an accurate extension of the SAFT-DFT approach.

Literature Cited

(1) Rowlinson, J. S.; Widom, B. Molecular Theory of Capillarity; Clarendon Press: Oxford, 1982.
(2) van der Waals, J. D. *Verhandel. Konink. Akad. Weten.* **1893**, *1*, 56; translated into English by Rowlinson, J. S. The thermodynamic theory of capillarity under the hypothesis of a continuous variation of density. *J. Stat. Phys.* **1979**, *20*, 197−244.
(3) Strutt, J. W. (Lord Rayleigh). On the theory of surface forces. II. Compressible fluids. *Philos. Mag.* **1892**, *33*, 209.
(4) Cahn, J. W.; Hilliard, J. E. Free Energy of a Nonuniform System. I. Interfacial Free Energy. *J. Chem. Phys.* **1958**, *28*, 258–266.
(5) Evans, R. *Density Functionals in the Theory of Nonuniform Fluids. Fundamentals of Inhomogeneous Fluids*; Dekker: New York, 1992.
(6) Chapela, G. A.; Saville, G.; Rowlinson, J. S. Computer simulation of the gas/liquid surface. *Faraday Discuss. Chem. Soc.* **1975**, *59*, 22–28.
(7) Chapela, G. A.; Saville, G.; Thompson, S. M.; Rowlinson, J. S. Computer simulation of a gas−liquid surface. Part 1. *J. Chem. Soc., Faraday Trans. 2* **1977**, *73*, 1133–1144.
(8) Thompson, S. M.; Gubbins, K. E.; Walton, J. P. R. B.; Chantry, R. A. R.; Rowlinson, J. S. A molecular dynamics study of liquid drops. *J. Chem. Phys.* **1984**, *81*, 530–542.
(9) Gloor, G. J.; Jackson, G.; Blas, F. J.; de Miguel, E. Test-area simulation method for the direct determination of the interfacial tension of systems with continuous or discontinuous potentials. *J. Chem. Phys.* **2005**, *123*, 134703–19.
(10) Kirkwood, J. G.; Buff, F. P. The statistical mechanical theory of surface tension. *J. Chem. Phys.* **1949**, *17*, 338–343.
(11) Binder, K. Monte Carlo calculation of the surface tension for two- and three-dimensional lattice-gas models. *Phys. Rev. A* **1982**, *25*, 1699–1709.
(12) Bennett, C. H. Efficient estimation of free energy differences from Monte Carlo data. *J. Comput. Phys.* **1976**, *22*, 245–268.
(13) Miyazaki, J.; Barker, J. A.; Pound, G. M. A new Monte Carlo method for calculating surface tension. *J. Chem. Phys.* **1976**, *64*, 3364–3369.
(14) Salomons, E.; Mareschal, M. Surface tension, adsorption and surface entropy of liquid-vapour systems by atomistic simulation. *J. Phys.: Condens. Matter* **1991**, *3*, 3645–3661.
(15) Zwanzig, R. W. High-temperature equation of state by a perturbation method. I. Nonpolar gases. *J. Chem. Phys.* **1954**, *22*, 1420–1426.
(16) Errington, J. R.; Kofke, D. A. Calculation of surface tension via area sampling. *J. Chem. Phys.* **2007**, *127*, 174709–12.
(17) de Miguel, E. Computation of surface tensions using expanded ensemble simulations. *J. Phys. Chem. B* **2008**, *112*, 4674–4679.
(18) MacDowell, L. G.; Bryk, P. Direct calculation of interfacial tensions from computer simulation: Results for freely jointed tangent hard sphere chains. *Phys. Rev. E* **2007**, *75*, 061609−13.
(19) Widom, B. Some topics in the theory of fluids. *J. Chem. Phys.* **1963**, *39*, 2808–2812.
(20) Eppenga, R.; Frenkel, D. Monte Carlo study of the isotropic and nematic phases of infinitely thin hard platelets. *Mol. Phys.* **1984**, *52*, 1303–1334.
(21) Harismiadis, V. I.; Vorholz, J.; Panagiotopoulos, A. Z. Efficient pressure estimation in molecular simulations without evaluating the virial. *J. Chem. Phys.* **1996**, *105*, 8469–8470.

(22) Vortler, H. L.; Smith, W. R. Computer simulation studies of a square-well fluid in a slit pore. Spreading pressure and vapor-liquid phase equilibria using the virtual-parameter-variation method. *J. Chem. Phys.* **2000**, *112*, 5168–5174.

(23) de Miguel, E.; Jackson, G. The nature of the calculation of the pressure in molecular simulations of continuous models from volume perturbations. *J. Chem. Phys.* **2006**, *125*, 164109–11.

(24) de Miguel, E.; Jackson, G. Detailed examination of the calculation of the pressure in simulations of systems with discontinuous interactions from the mechanical and thermodynamic perspectives. *Mol. Phys.* **2006**, *104*, 3717–3734.

(25) Ibergay, C.; Ghoufi, A.; Goujon, F.; Ungerer, P.; Boutin, A.; Rousseau, B.; Malfreyt, P. Molecular simulations of the *n*-alkane liquid-vapour interface: Interfacial properties and their long range corrections. *Phys. Rev. E* **2007**, *75*, 051602−18.

(26) Vega, C.; de Miguel, E. Surface tension of the most popular models of water by using the test-area simulation method. *J. Chem. Phys.* **2007**, *126*, 154707–10.

(27) Müller, E. A.; Mejía, A. Interfacial properties of selected binary mixtures containing *n*-alkanes. *Fluid Phase Equilib.* **2010**, *282*, 68–81.

(28) Biscay, F.; Ghoufi, A.; Lachet, V.; Malfreyt, P. Monte Carlo calculation of the methane-water interfacial tension at high pressures. *J. Chem. Phys.* **2009**, *131*, 124707–16.

(29) Biscay, F.; Ghoufi, A.; Lachet, V.; Malfreyt, P. Monte Carlo simulations of the pressure dependence of the water-acid gas interfacial tensions. *J. Phys. Chem. B* **2009**, *113*, 14277–14290.

(30) Ghoufi, A.; Goujon, F.; Lachet, V.; Malfreyt, P. Surface tension of water and acid gases from Monte Carlo simulations. *J. Chem. Phys.* **2008**, *128*, 154716–16.

(31) Pensado, A. S.; Malfreyt, P.; Pádua, A. A. H. Molecular dynamics simulations of the liquid surface of the ionic liquid 1-Hexyl-3-methylimidazolium Bis(trifluoromethanesulfonyl)amide: Structure and surface tension. *J. Phys. Chem. B* **2009**, *113*, 14708–14718.

(32) Blas, F. J.; MacDowell, L. G.; de Miguel, E.; Jackson, G. Vapor-liquid interfacial properties of fully flexible Lennard-Jones chains. *J. Chem. Phys.* **2008**, *129*, 144703–9.

(33) MacDowell, L. G.; Blas, F. J. Surface tension of fully flexible Lennard-Jones chains: Role of long-range corrections. *J. Chem. Phys.* **2009**, *131*, 074705−10.

(34) de Miguel, E.; Almarza, N. G.; Jackson, G. Surface tension of the Widom-Rowlinson model. *J. Chem. Phys.* **2007**, *127*, 034707−10.

(35) Galliero, G.; Pineiro, M.; Mendiboure, B.; Miqueu, C.; Lafitte, T.; Bessieres, D. Interfacial properties of the Mie *n*-6 fluid: Molecular simulations and gradient theory results. *J. Chem. Phys.* **2009**, *130*, 104704–10.

(36) Sampayo, J. G.; Malijevský, A.; Müller, E. A.; de Miguel, E.; Jackson, G. Communications: Evidence for the role of fluctuations in the thermodynamics of nanoscale drops and the implications in computations of the surface tension. *J. Chem. Phys.* **2010**, *132*, 141101–4.

(37) Wilson, M. R.; Allen, M. P. Computer simulation study of liquid crystal formation in a semi-flexible system of linked hard spheres. *Mol. Phys.* **1993**, *80*, 277–295.

(38) Williamson, D. C.; Jackson, G. Liquid crystalline phase behavior in systems of hard-sphere chains. *J. Chem. Phys.* **1998**, *108*, 10294–10302.

(39) Gil-Villegas, A.; McGrother, S. C.; Jackson, G. Reaction-field and Ewald summation methods in Monte Carlo simulations of dipolar liquid crystals. *Mol. Phys.* **1997**, *92*, 723–734.

(40) McGrother, S. C.; Gil-Villegas, A.; Jackson, G. The effect of dipolar interactions on the liquid crystalline phase transitions of hard spherocylinders with central longitudinal dipoles. *Mol. Phys.* **1998**, *95*, 657–673.

(41) van Duijneveldt, J. S.; Allen, M. P. Computer simulation study of a flexible-rigid-flexible model for liquid crystals. *Mol. Phys.* **1997**, *92*, 855–870.

(42) van Duijneveldt, J. S.; Gil-Villegas, A.; Jackson, G.; Allen, M. P. Simulation study of the phase behavior of a primitive model for thermotropic liquid crystals: Rodlike molecules with terminal dipoles and flexible tails. *J. Chem. Phys.* **2000**, *112*, 9092–9104.

(43) Bolhuis, P. G.; Louis, A. A.; Hansen, J.-P. Many-body interactions and correlations in coarse-grained descriptions of polymer solutions. *Phys. Rev. E* **2001**, *64*, 021801−12.

(44) Paricaud, P.; Varga, S.; Jackson, G. Study of the demixing transition in model athermal mixtures of colloids and flexible self-excluding polymers using the thermodynamic perturbation theory of Wertheim. *J. Chem. Phys.* **2003**, *118*, 8525–8536.

(45) Galindo, A.; Haslam, A. J.; Varga, S.; Jackson, G.; Vanakaras, A. G.; Photinos, D. J.; Dunmur, D. A. The phase behavior of a binary mixture of rodlike and disclike mesogens: Monte Carlo simulation, theory, and experiment. *J. Chem. Phys.* **2003**, *119*, 5216–5225.

(46) Cuetos, A.; Galindo, A.; Jackson, G. Thermotropic biaxial liquid crystalline phases in a mixture of attractive uniaxial rod and disk particles. *Phys. Rev. Lett.* **2008**, *101*, 237802–4.

(47) Trokhymchuk, A.; Alejandre, J. Computer simulations of liquid/vapor interface in Lennard-Jones fluids: Some questions and answers. *J. Chem. Phys.* **1999**, *111*, 8510–8523.

(48) Duque, D.; Pàmies, J. C.; Vega, L. F. Interfacial properties of Lennard-Jones chains by direct simulation and density gradient theory. *J. Chem. Phys.* **2005**, *121*, 11395–11401.

(49) Allen, M. P.; Tildesley, D. J. *Computer Simulation of Liquids*; Clarendon Press: Oxford, 1987.

(50) Gelb, L. D.; Müller, E. A. Location of phase equilibria by temperature-quench molecular dynamics simulations. *Fluid Phase Equilib.* **2002**, *203*, 1–14.

(51) Dubey, G. S.; O'Shea, S. F.; Monson, P. A. Vapour-liquid equilibria for two centre Lennard-Jones diatomics and dipolar diatomics. *Mol. Phys.* **1993**, *4*, 997–1007.

(52) Kriebel, C.; Müller, A.; Winkelmann, J.; Fischer, J. Vapour-liquid equilibria of two-centre Lennard-Jones fluids from the *NpT* plus test particle method. *Mol. Phys.* **1995**, *84*, 381–394.

(53) Vega, L.; de Miguel, E.; Rull, L. F.; Jackson, G.; McLure, I. A. Phase equilibria and critical behavior of square-well fluids of variable width by Gibbs ensemble Monte Carlo simulation. *J. Chem. Phys.* **1992**, *96*, 2296–2305.

(54) Guggenheim, E. A. *Thermodynamics*, 4th ed.; North Holland: Amsterdam, 1959.

(55) Kriebel, C.; Mecke, M.; Winkelmann, J.; Vrabec, J.; Fischer, J. An equation of state for dipolar two-center Lennard-Jones molecules and its application to refrigerants. *Fluid Phase Equilib.* **1998**, *142*, 15–32.

(56) Vrabec, J.; Stoll, J.; Hasse, H. A set of molecular models for symmetric quadrupolar fluids. *J. Phys. Chem. B* **2001**, *105*, 12126–12133.

(57) Singer, K.; Taylor, A.; Singer, J. V. L. Thermodynamic and structural properties of liquids modelled by '2-Lennard-Jones centres' pair potentials. *Mol. Phys.* **1977**, *33*, 1757–1795.

(58) Fischer, J.; Lustig, R.; Breitenfelder-Manske, H.; Lemming, W. Influence of intermolecular potential parameters on orthobaric properties of fluids consisting of spherical and linear molecules. *Mol. Phys.* **1984**, *52*, 485–497.

(59) Bohn, M.; Lustig, R.; Fischer, J. Description of polyatomic real substances by two-center Lennard-Jones model fluids. *Fluid Phase Equilib.* **1986**, *25*, 251–262.

(60) Kohler, F.; Nhu, N. V. The second virial coefficients of some halogenated ethanes. *Mol. Phys.* **1993**, *80*, 795–800.

(61) McGuigan, D. B.; Lupkowski, M.; Paquet, D. M.; Monson, P. A. Phase diagrams of interaction site fluids I. Homonuclear 12−6 diatomics. *Mol. Phys.* **1989**, *67*, 33–52.

(62) Spyriouni, T.; Economou, I. G.; Theodorou, D. N. Phase equilibria of mixtures containing chain molecules predicted through a novel simulation scheme. *Phys. Rev. Lett.* **1998**, *80*, 4466–4469.

(63) Mecke, M.; Müller, A.; Winkelmann, J.; Fischer, J. An equation of state for two-center Lennard-Jones fluids. *Int. J. Thermophys.* **1997**, *18*, 683–698.

(64) Lísal, M.; Aim, K.; Mecke, M. Fischer, Revised equation of state for two-center Lennard-Jones fluids. *Int. J. Thermophys.* **2004**, *25*, 159–173.

(65) *National Institute of Standards and Technology (NIST) Chemistry WebBook*, Thermophysical properties of fluid systems; NIST: Gaithersburg, MD. http://webbook.nist.gov/chemistry/ (accessed June 2010).

(66) Vargaftik, N. B. *Tables on the thermophysical properties of liquids and gases*, 2nd ed.; Wiley: New York, 1987.

(67) PROSIM, Component Plus 3.4; online free database software. http://www.prosim.net/ (accessed June 2010).

(68) Filipe, E. J. M.; Gomez de Azevedo, E. J. S.; Martins, L. F. G.; Soares, V. A. M.; Calado, J. C. G.; McCabe, C.; Jackson, G. Thermodynamics of liquid mixtures of xenon with alkanes: (xenon + ethane) and (xenon + propane). *J. Phys. Chem. B* **2000**, *104*, 1315–1321.

(69) Filipe, E. J. M.; Martins, L. F. G.; Calado, J. C. G.; McCabe, C.; Jackson, G. Thermodynamics of liquid mixtures of xenon with alkanes: (xenon + *n*-butane) and (xenon + isobutane). *J. Phys. Chem. B* **2000**, *104*, 1322–1325.

(70) Filipe, E. J. M.; Dias, L. M. B.; Calado, J. C. G.; McCabe, C.; Jackson, G. Is xenon an ennobled alkane? *Phys. Chem. Chem. Phys.* **2002**, *4*, 1618–1621.

(71) Blas, F. J.; del Rio, E. M.; de Miguel, E.; Jackson, G. An examination of the vapour-liquid interface of associating fluids using a SAFT-DFT approach. *Mol. Phys.* **2001**, *99*, 1851–1865.

(72) Gloor, G. J.; Blas, F. J.; del Rio, E. M.; de Miguel, E.; Jackson, G. A SAFT−DFT approach for the vapour−liquid interface of associating fluids. *Fluid Phase Equilib.* **2002**, *194*, 521–530.

(73) Gloor, G. J.; Jackson, G.; Blas, F. J.; del Rio, E. M.; de Miguel, E. An accurate density functional theory for the vapor-liquid interface of associating chain molecules based on the statistical associating fluid

theory for potentials of variable range. *J. Chem. Phys.* **2004**, *121*, 12740–12759.
(74) Gloor, G. J.; Jackson, G.; Blas, F. J.; del Rio, E. M.; de Miguel, E. Prediction of the vapor−liquid interfacial tension of nonassociating and associating fluids with the SAFT-VR density functional theory. *J. Phys. Chem. C* **2007**, *111*, 15513–15522.
(75) Llovell, F.; Galindo, A.; Blas, F. J.; Jackson, G. Classical density functional theory for the prediction of the surface tension and interfacial properties of fluids mixtures of chain molecules based on the statistical associating fluid theory for potentials of variable range. *J. Chem. Phys.* **2010**, *133*, 024704−19.
(76) Gil-Villegas, A.; Galindo, A.; Whitehead, P. J.; Mills, S. J.; Jackson, G.; Burgess, A. N. Statistical associating fluid theory for chain molecules with attractive potentials of variable range. *J. Chem. Phys.* **1997**, *106*, 4168–4186.
(77) Galindo, A.; Davies, L. A.; Gil-Villegas, A.; Jackson, G. The thermodynamics of mixtures and the corresponding mixing rules in the SAFT-VR approach for potentials of variable range. *Mol. Phys.* **1998**, *93*, 241–252.
(78) Davies, L. A.; Gil-Villegas, A.; Jackson, G. Describing the properties of chains of segments interacting via soft-core potentials of variable range with the SAFT-VR approach. *Int. J. Thermophys.* **1998**, *19*, 675–686.
(79) Davies, L. A.; Gil-Villegas, A.; Jackson, G. An analytical equation of state for chain molecules formed from Yukawa segments. *J. Chem. Phys.* **1999**, *111*, 8659–8665.
(80) Lafitte, T.; Bessieres, D.; Piñeiro, M. M.; Daridon, J. L. Simultaneous estimation of phase behavior and second-derivative properties using the statistical associating fluid theory with variable range approach. *J. Chem. Phys.* **2006**, *124*, 024509−16.

Received for review April 30, 2010. Accepted June 14, 2010. J.G.S. acknowledges financial support from the Consejo Nacional de Ciencia y Tecnología (CONACYT) of Mexico for a Ph.D. studentship. E.dM. is grateful for funding from Project No. FIS2007-66079-CO2-02 of the Spanish Dirección General de Investigación. F.J.B. acknowledges financial support from Project No. FIS2010-14866 of the Spanish Dirección General de Investigación, from the Proyecto de Excelencia of the Junta de Andalucía (Project No. P07-FQM02884) and from the Universidad de Huelva and Junta de Andalucía. We also gratefully acknowledge funding from the Engineering and Physical Sciences Research Council (EPSRC, Grant No. EP/E016340) of the United Kingdom.

JE100450S